

Multiscale Gentlest Ascent Dynamics

Xiang Zhou ¹, Shuting Gu
 Department of Mathematics
 City University of Hong Kong
 Tat Chee Ave, Kowloon
 Hong Kong SAR

ABSTRACT

The gentlest ascent dynamics (E and Zhou in *Nonlinearity* vol 24, p1831, 2011) locally converges to a nearby saddle point with one dimensional unstable manifold. Here we present a multiscale gentlest ascent dynamics for stochastic slow-fast systems in order to compute saddle point associated with the effective dynamics of the slow variable. Such saddle points, as the candidates of transition states, are important in non-equilibrium transitions for the coarse-grained slow variables; they are also helpful to explore free energy surface. We derive the expressions of the gentlest ascent dynamics for the averaged system, and propose the multiscale numerical methods to efficiently solve the multiscale gentlest ascent dynamics for search of saddle point. The examples of stochastic ordinary and partial differential equations are presented to illustrate the performance of this multiscale gentlest ascent dynamics.

Keywords: saddle point, gentlest ascent dynamics, multiscale method

Mathematics Subject Classification (2010) Primary 65K05, Secondary 82B05

1. INTRODUCTION

The following slow-fast system $(X(t), Y(t)) \in \mathcal{X} \times \mathcal{Y}$ is a typical dynamic system with two disparate time scales:

$$\begin{cases} \dot{X}^\varepsilon(t) = f(X^\varepsilon, Y^\varepsilon), & (1a) \\ \dot{Y}^\varepsilon(t) = \frac{1}{\varepsilon}b(X^\varepsilon, Y^\varepsilon) + \frac{1}{\sqrt{\varepsilon}}\sigma(X^\varepsilon, Y^\varepsilon)\eta(t), & (1b) \end{cases}$$

where ε is a small parameter. X^ε is slow variable and Y^ε is fast variable. For simplicity, we assume $\mathcal{X} = \mathbb{R}^n$ and $\mathcal{Y} = \mathbb{R}^m$. The functions $f(x, y) = (f_1, f_2, \dots, f_n) : \mathbb{R}^n \times \mathbb{R}^m \rightarrow \mathbb{R}^n$ and $b(x, y) = (b_1, b_2, \dots, b_m) : \mathbb{R}^n \times \mathbb{R}^m \rightarrow \mathbb{R}^m$ are two smooth vector fields. The $m \times m$ diffusion matrix $\sigma(x, y)$ is assumed non-degenerate for all x and y . $\eta(t)$ is the zero-mean Gaussian noise in \mathbb{R}^m with certain covariance function $E(\eta(t)\eta(t'))$. For example, $E(\eta(t)\eta(t')) = \delta(t - t')$

¹email: xiang.zhou@city.edu.hk. The research of XZ was supported by the grants from the Research Grants Council of the Hong Kong Special Administrative Region, China (Project No. CityU 11304314, 109113 and 11304715).

means η is a white noise \dot{W} . We only consider this white noise case in this paper since the specific types of noise is not the main concern of this note.

Many interests for the above multiscale system concern the effective dynamics of the slow variable if the fast dynamics can be slaved and eliminated as the parameter ε tends to zero. Indeed, for any fixed $T < \infty$, the slow variable of (1), $X^\varepsilon(t)$, converges to a deterministic function $\bar{X}(t)$ satisfying an averaged equation,

$$\dot{\bar{X}}(t) = F(\bar{X}(t)),$$

during the time interval $t \in [0, T]$, for some function $F : \mathcal{X} \rightarrow \mathbb{R}$. Under certain stronger conditions, this convergence is also uniform in T . This is the typical result of the averaging principle, which has been developed in many classic mathematical literature (see [19, 27, 20] and the books [6, 12]). On the application side, one of the most important example is the *extended Lagrangian method* for the coarse-grained molecular dynamics (refer to [17, 32] and [6]). In this application, the slow variable X is usually the coarse-grained variables (collective variables) to describe the macroscopic features of the underlying complex system and the fast variable Y corresponds to the microscopic variables of full atomistic coordinates. To map the full complex energy surface in \mathcal{Y} into a low dimensional free energy surface in \mathcal{X} , it is essential to solve the averaged dynamics of the coarse-grained variable \bar{X} with efficient numerical methods such as the heterogeneous multiscale method (HMM) in [7, 8, 32].

However, for the metastability in the slow-fast system when there exist multiple wells or attractors in the effective dynamics $\dot{\bar{X}} = F(\bar{X})$, the behaviour of the random process X^ε on large time interval is more important. The difference of $X^\varepsilon - \bar{X}$ will be significantly large to escape the basin of attraction if the waiting time is sufficiently long. This type of large deviation result for the slow-fast system [30, 3] is analogous to the classic Freidlin-Wentzell theory [12] for the dynamic system perturbed by additive vanishing noise. There exists an exponentially large time scale responsible for the rare hoppings of X^ε between the metastable states in the space \mathcal{X} . To bridge this huge time scale gap, many methods have been proposed. For example, the metadynamics suggested by Iannuzzi, Laio and Parrinello in [17, 22], as a sampling method, introduced non-Markovian memory term into the extended Lagrangian method to discourage the trajectory from going back to old regions which have been visited. The authors in [25] combined the idea of the string method for minimum energy path ([5]) and the HMM for the multiscale sampling and developed new techniques to compute the minimum free energy paths in the relatively low dimensional space \mathcal{X} .

In this paper, we focus on the calculation of saddle points for the averaged system in space \mathcal{X} . From the perspective of the large deviation principle [12, 3] for the slow-fast system (1), there are little discussions on the connection of optimal transition paths with saddle points (particularly for the general dynamics without energy landscape), as compared to the case of additive small noise ([34]). However, the search of saddle points is critically useful in practice

for exploration of the boundary of attraction basin or the free energy surface. In addition, the computational cost of saddle point search generally is much cheaper than that of the optimization in path space based on the least action principle. The multiscale gentlest ascent dynamics (“MsGAD”) we develop here will directly target toward the saddle points on the basin boundary of metastable state in effective dynamics and offer a straightforward route of escaping the attraction basin.

Specifically, we are interested in index-1 saddle points for the effective dynamics associated with the slow-fast system (1). By index-1, we mean that the unstable manifold of the flow F at the saddle point is one dimensional. For high index case, our method is also applicable after modified properly as in the paper of the traditional GAD ([10]). The applicability of the GAD is not limited to gradient system. The original motivation of the GAD is based on the min-mode or eigenvector-following methodology (see, e.g., [4, 31]). The numerical developments based on this methodology, such as the dimer method([16]), the activation-relaxation techniques ([26]), etc., have been used for quite a few applications on potential energy surface. The applications of the GAD include [28, 11, 24]. The authors in [2, 1] have some further discussions on the properties of the GAD. As an acceleration technique for the GAD, a new iterative formulation and its algorithmic implementation for gradient system has been recently developed in [13] and [14], respectively. One of the advantages of the GAD is that its form is a continuous-time dynamic system, so it is very easy to fit in our current framework for the slow-fast dynamics (1). The application of GAD to sample the free energy surface has been discussed in [29] by Samanta *et al* for temperature-accelerated molecular dynamics. Our work here on the multiscale GAD (MsGAD) is a mathematical generalization of [29] and serves as an extensive discussion of the multiscale computations on the GAD for the slow-fast system.

The organization of the paper is as follows. In Section 1.1 and Section 1.2, we recall the averaging theorem for the slow-fast system (1) and the gentlest ascent dynamics. In Section 2 we derive the gentlest ascent dynamics for the averaged system, develop the multiscale methods for computations and discuss the algorithmic details, followed by a remark on the connection to central limit result. Section 3 is devoted to the gradient system where an extended potential energy function exists, in view of the practical importance of this class of models. Two examples are presented in Section 4 to demonstrate our method and the concluding remarks are given in Section 5.

1.1. Averaging principle of slow-fast stochastic dynamics. The averaging principle to derive the effective dynamics for the slow-fast system (1) is based on the ergodicity assumption of the fast process Y^ε . Let \tilde{Y}^x be the solution of the equation

$$\dot{\tilde{Y}}^x = b(x, \tilde{Y}^x) + \sigma(x, \tilde{Y}^x)\eta(t), \quad (2)$$

for any fixed parameter x . This is named as the virtually fast process. Assume that the virtually fast process \tilde{Y}^x is ergodic at every x and its unique invariant measure $\mu_x(dy)$ has a density function $\rho(x, y)$:

$$\mu_x(dy) = \rho(x, y)dy = \frac{1}{Z(x)}e^{-U(x,y)}dy, \quad (3)$$

where the normalization factor $Z(x)$ is

$$Z(x) \doteq \int e^{-U(x,y)}dy. \quad (4)$$

Remark 1. *If $b(x, y) = -\nabla_y U_1(x, y)$ and $\sigma(x, y) \equiv \sigma I$ for some potential energy function $U_1(x, y)$ and a constant σ , i.e., the fast dynamics is a gradient system, then $U(x, y) = \frac{2}{\sigma^2}U_1(x, y)$ and the equilibrium distribution $\rho(x, y) = e^{-\frac{2}{\sigma^2}U_1(x,y)} / \int e^{-\frac{2}{\sigma^2}U_1(x,y)}dy$. Otherwise, we can only simply set $U(x) = -\log \rho(x, y)$ and $Z(x) \equiv 1$.*

By the ergodicity assumption, for any integrable function u , the expectation with respect to μ_x can be estimated by the time average,

$$\int u(y)\mu_x(dy) = \lim_{T \rightarrow \infty} \frac{1}{T} \int_0^T u(\tilde{Y}(t))dt.$$

The averaging principle (cf. [6, 12] and references therein) states that as $\varepsilon \downarrow 0$, the slow component of the system (1), $X^\varepsilon(t)$, has a limit $\bar{X}(t)$ satisfying the following ordinary differential equation,

$$\dot{\bar{X}} = F(\bar{X}), \quad \text{where } F(x) \doteq \int f(x, y)\mu_x(dy). \quad (5)$$

In most cases the averaging function F above has no closed formula, and the solution \bar{X} has to be approximated by the numerical methods. Refer to the book [6] for an excellent summary of multiscale methods for this slow-fast dynamics.

1.2. Gentlest Ascent Dynamics (GAD). For a dynamic system $\dot{x}(t) = \varphi(x(t))$ where the flow φ is C^2 -smooth, the gentlest ascent dynamics locally converges to saddle point of φ by coupling position variable and direction variable. This dynamics, as a solution to the saddle point problem, can be viewed as a counterpart to the steepest descent dynamics for searching local minima. In this note, we are only interested in the index-1 saddle point, i.e., the unstable manifold of the saddle point is one dimensional.

The GAD for the flow $\dot{x}(t) = \varphi(x(t))$ is the following extended system for (x, v, w) ,

$$\begin{cases} \dot{x}(t) = \varphi(x) - 2 \frac{\langle \varphi(x), w \rangle}{\langle w, v \rangle} v, & (6a) \\ \gamma \dot{v}(t) = D\varphi(x)v - \alpha v, & (6b) \\ \gamma \dot{w}(t) = D\varphi(x)^\top w - \beta w, & (6c) \end{cases}$$

where $\langle \cdot, \cdot \rangle$ is the inner product, $D\varphi(x)$ is the Jacobi matrix $(D\varphi)_{ij} \doteq \frac{\partial \varphi_i}{\partial x_j}$. Two scalars α and β are Lagrangian multipliers to impose certain normalization conditions for v and w . For instance, if one uses the normalization condition $\langle v, v \rangle = \langle w, w \rangle = 1$, then $\alpha = \langle v, D\varphi(x)v \rangle$ and $\beta = 2 \langle w, D\varphi(x)v \rangle - \alpha$. By setting $\langle v(0), v(0) \rangle = \langle w(0), w(0) \rangle = 1$, the GAD flow (6) for such choices of α and β then will preserve these two normalization equations. This technique to determine α and β will be applied later in many same situations; we shall not repeat the calculation of these Lagrangian multipliers.

The modified force in (6a) has the effect of inverting the direction of the original force $\varphi(x)$ on the direction v to sustain ‘‘ascent’’ flow around the index-1 saddle point. The dynamics (6b) and (6c), if x is frozen and as time goes to infinity, tend to the left-eigenvector w and the right-eigenvector v of the Jacobi $D\varphi(x)$ corresponding to the largest eigenvalue, respectively. The coupling of x and (v, w) is actually relaxed by a finite positive number γ in (6), which introduces a separation of time scale artificially. As $\gamma \downarrow 0$, equation (6) becomes a two-scale system where x is slow variable and (v, w) are fast variables. When the fast variables v and w have a single limit state as time goes to infinity, denoted by $v(x)$ and $w(x)$, respectively, then $v(x)$ and $w(x)$ are the right and left eigenvector of $D\varphi(x)$. In this case, at the limit $\gamma \downarrow 0$, the effective dynamics of (6) is

$$\dot{x}(t) = \varphi(x) - 2 \frac{\langle \varphi(x), w(x) \rangle}{\langle v(x), w(x) \rangle} v(x). \quad (7)$$

The rigorous proof of the local convergence of the GAD (6) to a nearby index-1 saddle point is presented in [10] for any finite γ and in the appendix of [14] for the limit of vanishing γ .

Since the Jacobi matrix $D\varphi$ is generally asymmetric, the right directions v and the left direction w are both required in (6) to obliquely project the force φ onto $span\{v\}$ and $span\{v\}^\perp$, except for gradient system $\varphi(x) = -\nabla V(x)$, where the Hessian is symmetric. The GAD for gradient system involves only v :

$$\begin{cases} \dot{x}(t) = -\nabla V(x) + 2 \frac{\langle \nabla V(x), v \rangle}{\langle v, v \rangle} v, & (8a) \\ \gamma \dot{v}(t) = -\nabla^2 V(x)v + \langle v, \nabla^2 V(x)v \rangle v, & (8b) \end{cases}$$

where $\nabla^2 V$ is the Hessian matrix of potential energy function $V(x)$. The equation (8b) is in fact the steepest descent flow (rescaled by γ) to minimize the Rayleigh quotient, $\min_{\|v\|=1} v^\top H v$, for the Hessian matrix $H \doteq \nabla^2 V(x)$. So,

the steady state $v(x)$ is actually the eigenvector of the Hessian H at the lowest eigenvalue, the so called “min-mode”.

In evolving the vector $v(t)$ in (8b), it may not need the full Hessian matrix in practice. The computation of the Hessian-vector multiplication $\nabla^2 V(x)v$ is usually done by the finite difference method as in the dimer method ([16, 33]), because this multiplication is exactly the directional derivative along the v direction:

$$\nabla^2 V(x)v = \frac{d}{dh} \nabla V(x + hv)|_{h=0} \approx h^{-1}(\nabla V(x + hv) - \nabla V(x)).$$

2. MULTISCALE GENTLEST ASCENT DYNAMICS FOR SLOW-FAST SYSTEM

2.1. Formulation of GAD for slow-fast system. We intend to extend the GAD to the slow-fast dynamics (1) to calculate index-1 saddle points of the effective flow $\dot{\bar{X}} = F(\bar{X})$ defined in (5). The direct application of the GAD (6) to equation (5) immediately gives

$$\begin{cases} \dot{x}(t) = F(x) - 2 \frac{\langle F(x), w \rangle}{\langle v, w \rangle} v, & (9a) \\ \gamma \dot{v}(t) = DF(x)v - \alpha v, & (9b) \\ \gamma \dot{w}(t) = DF(x)^\top w - \beta w, & (9c) \end{cases}$$

where $F(x) = \int f(x, y)\rho(x, y)dy$ by definition, and $DF(x)$ is the Jacobi matrix of $F(x)$. Note the density $\rho(x, y) = Z(x)^{-1}e^{-U(x, y)}$. We introduce

$$g(x, y) \doteq -\nabla_x U(x, y), \quad (10)$$

and

$$G(x) \doteq \int g(x, y)\rho(x, y)dy. \quad (11)$$

By the definition of $Z(x)$ in (4), we simply see

$$\nabla_x \log Z(x) = Z^{-1}(x)\nabla_x Z(x) = \int g(x, y)\rho(x, y)dy = G(x). \quad (12)$$

We calculate the Jacobi matrix as follows,

$$\begin{aligned} (DF)_{ij}(x) &= \frac{\partial F_i}{\partial x_j}(x) = \frac{\partial}{\partial x_j} \left(\int f_i(x, y)Z^{-1}(x)e^{-U(x, y)}dy \right) \\ &= \int (\partial_{x_j} f_i(x, y) + f_i(x, y)g_j(x, y) - f_i(x, y)\partial_{x_j} Z(x)Z^{-1}(x)) \rho(x, y)dy \\ &= \int (\partial_{x_j} f_i(x, y) + f_i(x, y)g_j(x, y) - f_i(x, y)G_j(x)) \rho(x, y)dy \\ &= \overline{\partial_{x_j} f_i(x)} + \overline{f_i g_j(x)} - F_i(x)G_j(x). \end{aligned}$$

To ease presentation, the overlined symbol $\bar{\theta}(x)$ for a bivariate function $\theta(x, y)$ is used to define the expectation with respect to $\mu_x(dy)$, that is,

$$\bar{\theta}(x) \doteq \int \theta(x, y) \mu_x(dy).$$

So, $\bar{f}(x) = F(x)$ and $\bar{g}(x) = G(x)$ by this definition.

The Jacobi matrix of the effective dynamics is thus given by

$$DF(x) = \overline{D_x f}(x) + \overline{C}(x) \quad (13)$$

where $D_x f(x, y)$ is the Jacobi matrix of $f(x, y)$ with respect to the variable x and

$$C(x, y) \doteq f \otimes g(x) - F(x) \otimes G(x). \quad (14)$$

The tensor product $u \otimes v$ for any two vectors u and v corresponds to the matrix $[u_i v_j]$.

The term $\overline{C}(x)$ in (13) comes from the x -dependency of the equilibrium distribution $\mu_x(dy)$. $\overline{C}(x)$ actually is the covariance of f and g w.r.t. the distribution $\mu_x(dy)$ because it is easy to verify that $\overline{C}(x) = \overline{(f - F) \otimes (g - G)}(x)$.

2.2. The Multiscale GAD. We shall address how to construct multiscale schemes for the system (9). We have obtained the expression of the Jacobi DF in (13), which is an ensemble average of the matrix $D_x f + C$ w.r.t. μ_x . This important feature allows us to view the system (9) as an averaged equation of a multiscale system involving the original fast variable y^ε :

$$\begin{cases} \dot{x}^\varepsilon(t) = f(x^\varepsilon, y^\varepsilon) - 2 \frac{\langle f(x^\varepsilon, y^\varepsilon), w^\varepsilon \rangle}{\langle w^\varepsilon, v^\varepsilon \rangle} v^\varepsilon, & (15a) \\ \dot{y}^\varepsilon(t) = \frac{1}{\varepsilon} b(x^\varepsilon, y^\varepsilon) + \frac{\sigma(x^\varepsilon, y^\varepsilon)}{\sqrt{\varepsilon}} \eta(t), & (15b) \\ \gamma \dot{v}^\varepsilon(t) = (D_x f(x^\varepsilon, y^\varepsilon) + C(x^\varepsilon, y^\varepsilon)) v^\varepsilon - \alpha^\varepsilon v^\varepsilon, & (15c) \\ \gamma \dot{w}^\varepsilon(t) = (D_x f(x^\varepsilon, y^\varepsilon) + C(x^\varepsilon, y^\varepsilon))^\top w^\varepsilon - \beta^\varepsilon w^\varepsilon. & (15d) \end{cases}$$

where the Lagrangian multipliers α^ε and β^ε can be defined accordingly as before to enforce certain normalization conditions. Here for any constant γ , as $\varepsilon \rightarrow 0$, the slow variables are $(x^\varepsilon, v^\varepsilon, w^\varepsilon)$ and the fast variable is y^ε . We name the multiscale system like (15) as the MsGAD (multiscale gentlest ascent dynamics). Notice that the covariance term C is rank-1, so the matrix-vector multiplication is actually calculated simply as the inner product calculation, for instance, $C(x, y)v = \langle g(x, y), v \rangle f(x, y) - \langle G(x), v \rangle F(x)$.

Remark 2. In the expression of $C(x, y) = f(x, y) \otimes g(x, y) - F(x) \otimes G(x)$, the averaged terms $F = \bar{f}$ and $G = \bar{g}$ have already involved the invariant measure μ_x , hence, the equations (9) and (15) are not in the “standard” forms like the equations (5) and (1) defined in Section 1.1. There is no much difference if the HMM is used (see below). But in the use of the seamless coupling method, to make the system (15) “standard”, one need introduce another process \hat{Y}_t^x as an

independent copy of the process \tilde{Y}_t^x to calculate the expectation for F first, then the expectation for $\bar{C} = \overline{f \otimes g - F \otimes g}$ is calculated from \tilde{Y}_t^x as before. This approach is based on the equivalent form of \bar{C} :

$$\bar{C}(x) = \int \left[f(x, y) \otimes g(x, y) - \left(\int f(x, y) \hat{\mu}_x(dy) \right) \otimes g(x, y) \right] \mu_x(dy),$$

where $\hat{\mu}_x (= \mu_x)$ is the equilibrium distribution of the iid copy \hat{Y}^x .

2.2.1. *HMM*. Now we discuss the framework of the HMM (*heterogeneous multiscale method*, [7, 8]) for our averaged GAD system (9) and the MsGAD (15). There are two parameters ε and γ in the multiscale GAD. We let ε tend to zero in (15) to obtain the equation (9) by the averaging principle. We can also further select a small γ in (9) to obtain an equation like (7).

The procedures of the HMM for the MsGAD are as follows. Select a macroscopic time step size Δt for evolving x and $\Delta\tau$ for evolving v and w (usually $\Delta\tau = \Delta t$); select a microscopic time step size δt for evolving y . The HMM scheme with forward Euler consists of the following

- (1) Use the macro-solver

$$x_{n+1} = x_n + (F_n - 2v_n \langle F_n, v_n \rangle / \langle w_n, v_n \rangle) \Delta t$$

where x_n is the approximation value of $\bar{X}(n\Delta t)$ and F_n, v_n, w_n are estimated below.

- (2) Apply the micro-solver with time step size δt for M micro-steps for the fast dynamics

$$y_{n,m+1} = y_{n,m} + \frac{\delta t}{\varepsilon} b(x_n, y_{n,m}) + \frac{\sigma(x_n, y_{n,m})}{\sqrt{\varepsilon}} \sqrt{\delta t} \eta_{n,m},$$

$m = 0, 1, 2, \dots, M-1$. Here $\{\eta_{n,m}\}$ are iid $\mathcal{N}(0, 1)$ random variables. The initial $y_{n,0} = y_{n-1,M}$.

- (3) Estimate F_n, G_n and the Jacobi matrix $(DF)_n$:

$$F_n = \frac{1}{M} \sum_{m=1}^M f(x_n, y_{n,m}), \quad G_n = \frac{1}{M} \sum_{m=1}^M g(x_n, y_{n,m}),$$

$$(DF)_n = \frac{1}{M} \sum_{m=1}^M \left(D_x f(x_n, y_{n,m}) + f(x_n, y_{n,m}) \otimes g(x_n, y_{n,m}) \right) - F_n \otimes G_n$$

- (4) Solve the right and left direction v_n and w_n for K steps by using the time step $\Delta\tau$ and the initial $v_{n,0} = v_{n-1}, w_{n,0} = w_{n-1}$:

$$\hat{v}_{n,k+1} = v_{n,k} + \Delta\tau (DF)_n v_{n,k}, \quad \hat{w}_{n,k+1} = w_{n,k} + \Delta\tau (DF)_n^\top w_{n,k},$$

$$v_{n,k+1} = \frac{\hat{v}_{n,k+1}}{|\hat{v}_{n,k+1}|}, \quad w_{n,k+1} = \frac{\hat{w}_{n,k+1}}{\langle v_{n,k+1}, \hat{w}_{n,k+1} \rangle}$$

$k = 0, 1, 2, \dots, K-1$. Then $v_n = v_{n,K}$ and $w_n = w_{n,K}$.

The microscopic time step size has to be much smaller than ε ; $\delta t/\varepsilon$ is the effective step size in solving the virtually fast process \tilde{Y} . The time length, $M \times \delta t$, should be sufficient long for the fast process Y^ε to relax toward the equilibrium distribution. The number of steps M also should be very large to reduce the statistical error in estimating the averaged quantities F , G and DF . The number of steps K is to take care of a possible small constant γ . $K = 1$ actually works in principle for many cases. A larger K can give a better accuracy for eigenvector, although it also has more computational burden. There is no requirement for $\Delta\tau$ as long as the ODE solver is stable; the time step size $\Delta\tau$ can be simply set as Δt .

Remark 3. *On the choice of the macro- solver for x and v, w , an explicit scheme with larger stability region is preferred, such as the stabilized Runge-Kutta methods. On the micro- solver for the virtually fast process, a numerical scheme for SDE with higher order weak convergence rate for the long time integration is preferred to capture the equilibrium distribution better. For instance, when σ is a constant, one can use the stochastic Heun method ([21]) which requires two force evaluations at each timestep or a non-Markovian scheme proposed recently in [23]:*

$$y_{n,m+1} = y_{n,m} + \frac{\delta t}{\varepsilon} b(x_n, y_{n,m}) + \frac{\sigma\sqrt{\delta t}}{2\sqrt{\varepsilon}} (\eta_{n,m} + \eta_{n,m+1}), \quad m = 0, 1, \dots$$

$\{\eta_{n,m}\}$ are iid $\mathcal{N}(0, 1)$ random variables.

2.2.2. Seamless coupling scheme. The seamless coupling strategy proposed in [9] does not need the back and forth communication of the macro- and micro-states of the system. It is essentially a boosting algorithm: by increasing the small parameter ε to a larger number ε' in the slow-fast system, the seamless scheme simultaneously solves this boosted system with the time step size $\tilde{\Delta}t$ which is smaller than the macro-time step size Δt in the HMM. It is potentially more efficient than the HMM if the micro-model is difficult. Following this idea, we increase ε in (15) to a larger number, say $\varepsilon' = \varepsilon\lambda$ for a constant $\lambda > 1$. As stated in Remark 2, we need introduce an independent copy z^ε for the fast process to handle the double expectation in the covariance matrix \overline{C} . In summary, the seamless coupling method solves the following system:

$$\left\{ \begin{array}{l} \dot{x}^\varepsilon(t) = f(x^\varepsilon, y^\varepsilon) - 2 \frac{\langle f(x^\varepsilon, y^\varepsilon), w^\varepsilon \rangle}{\langle w^\varepsilon, v^\varepsilon \rangle} v^\varepsilon, \\ \dot{y}^\varepsilon(t) = \frac{1}{\varepsilon\lambda} b(x^\varepsilon, y^\varepsilon) + \frac{1}{\sqrt{\varepsilon\lambda}} \eta_1(t), \\ \dot{z}^\varepsilon(t) = \frac{1}{\varepsilon\lambda} b(x^\varepsilon, z^\varepsilon) + \frac{1}{\sqrt{\varepsilon\lambda}} \eta_2(t), \\ \tau \dot{v}^\varepsilon(t) = (D_x f(x^\varepsilon, y^\varepsilon)) v^\varepsilon + f(x^\varepsilon, y^\varepsilon) \langle g(x^\varepsilon, y^\varepsilon), v^\varepsilon \rangle \\ \quad - f(x^\varepsilon, z^\varepsilon) \langle g(x^\varepsilon, y^\varepsilon), v^\varepsilon \rangle - \alpha^\varepsilon v^\varepsilon, \\ \tau \dot{w}^\varepsilon(t) = (D_x f(x^\varepsilon, y^\varepsilon))^\top w^\varepsilon + g(x^\varepsilon, y^\varepsilon) \langle f(x^\varepsilon, y^\varepsilon), w^\varepsilon \rangle \\ \quad - g(x^\varepsilon, z^\varepsilon) \langle f(x^\varepsilon, y^\varepsilon), w^\varepsilon \rangle - \beta^\varepsilon w^\varepsilon, \end{array} \right. \quad \begin{array}{l} (16a) \\ (16b) \\ (16c) \\ (16d) \\ (16e) \end{array}$$

where η_1 and η_2 are two iid copies of η . The joint fast processes y^ε and z^ε correspond to the equilibrium density $\mu_x(dy) \times \mu_x(dz)$. It is clear that as $\varepsilon \rightarrow 0$, the effective dynamics of (16) is just equation (9). The system (16) is solved by ODE/SDE solvers with a common time step size $\tilde{\Delta}t$ for all five components. [6] suggests a time step size $\tilde{\Delta}t = \Delta t/M$, where M is the micro-step number previously used in the HMM. After a sufficient long time for relaxation, the solution $x^\varepsilon(t)$ will go close to the index-1 saddle point of the flow F , then one may average $x^\varepsilon(t)$ within a time interval to improve the accuracy.

The difference between the HMM and the seamless coupling may be more transparent from the two forms of the GAD, equation (6) and equation (7), for the usual dynamic system $\dot{x} = \varphi(x)$. Equation (7) is in a form of ‘‘averaged’’ equation and is solved through precomputing the eigenvectors $v(x)$ and $w(x)$ by any numerical method such as the Lancos method or Conjugate Gradient method. This corresponds to the HMM idea, although no Monte Carlo sampling is needed for this case. In contrast, the canonical form of the GAD in equation (6) is a concurrent coupling of position and direction, via the non-vanishing parameter τ . This is clearly a seamless coupling strategy.

2.3. Numerical calculation of the right direction v . In the algorithms presented above, we formally use the full matrix of the Jacobi DF in the dynamics for the right and left directions $v(t)$ and $w(t)$. However, in most real applications, it is not efficient or even feasible to store this Jacobi matrix element by element. In what follows, we discuss this challenge and the numerical remedies according to the specific features of slow-fast system. We start from the right direction v . It is noted that in many cases, the dimension of \mathcal{X} is much lower than the dimension of \mathcal{Y} . This means that $D_x f(x, y)$ is a small scale matrix and its all entry-wise values can be calculated and stored with reasonable cost.

If the fast dynamics is of gradient type, i.e., $b(x, y) = -\nabla_y U_1(x, y)$ and $\sigma(x, y) \equiv \sigma I$, then $U = \frac{2}{\sigma^2} U_1$ and $g(x, y) = -\frac{2}{\sigma^2} \nabla_x U_1(x, y)$. The covariance matrix is $C(x, y) = -\frac{2}{\sigma^2} f(x, y) \otimes \nabla_x U_1(x, y)$. Assume the analytic form of

$\nabla_x U_1(x, y)$ is available in practice, then the rank-1 matrix C is easy to calculate: $C(x, y)v = -\frac{2}{\sigma^2}f(x, y)\langle \nabla_x U_1(x, y), v \rangle$.

However, for non-gradient dynamics, the equilibrium distribution $\rho(x, y)$ has no closed formula available. For the dynamics of v in (15c), the finite difference scheme

$$(17) \quad \begin{aligned} (DF(x))v &= \lim_{h \rightarrow 0} (F(x + hv) - F(x))/h, \\ &= \lim_{h \rightarrow 0} h^{-1} \int f(x + hv, y)\rho(x + hv, y) - f(x, y)\rho(x, y)dy, \end{aligned}$$

can be applied to compute the matrix-vector multiplication $(DF(x))v$. If one knows the closed form of the Jacobi matrix $D_x f$, $(D_x f(x, y))v$ thus can be directly computed by the matrix-vector multiplication. The remaining term $(DF - D_x f)v = \bar{C}(x)v$ can be computed by the finite difference scheme. By Remark 1 and equations (10) and (12), we have $g = \nabla_x \log \rho$ and $C(x, y) = f(x, y) \otimes (\nabla_x \log \rho(x, y)) = \rho^{-1}f(x, y) \otimes (\nabla_x \rho(x, y))$. Then,

$$\begin{aligned} C(x, y)v &= \rho^{-1}f(x, y)\langle v, \nabla_x \rho(x, y) \rangle \\ &= \rho^{-1}f(x, y) \lim_{h \rightarrow 0} (\rho(x + hv, y) - \rho(x, y))/h. \end{aligned}$$

It follows that

$$(18) \quad \begin{aligned} \bar{C}(x)v &= \int C(x, y)v\rho(x, y)dy \\ &= \lim_{h \rightarrow 0} h^{-1} \int f(x, y)(\rho(x + hv, y) - \rho(x, y))dy. \end{aligned}$$

So, (17) can be rewritten as:

$$(DF(x))v = \int D_x f(x, y)v\rho(x, y)dy + \lim_{h \rightarrow 0} h^{-1} \int f(x, y)(\rho(x + hv, y) - \rho(x, y))dy. \quad (19)$$

In practice, a finite size step h is used in (17) or (19). Then, in the MsGAD, besides the process \tilde{Y}_t^x slaved at x , a second independent virtually fast process \tilde{Y}_t^{x+hv} is also required to obtain the distribution $\rho(x + hv, \cdot)$. The integration in (19) is computed from the time averages from $\rho(x + hv, \cdot)$ and $\rho(x, \cdot)$.

2.4. Numerical calculation of the left direction w . In many cases, we have to evolve the dynamics for w direction in (15d), except that the original slow-fast system (1) is of the gradient type jointly (see Section 3 below). It is worthwhile to note that even if both the slow and the fast components are of (parametrized) gradient types separately, while the coupled system (1) is not jointly driven by a single potential energy function, then the resulted averaging equation (5) might still not be a gradient system and the Jacobi matrix $DF(x)$ is neither symmetric. Refer to Section 4.1 for such an example.

If the fast dynamics is gradient, as we mentioned above for $C(x, y)v$ calculation, it is also quite simple to calculate $C(x, y)^T w$ by using $\nabla_x U_1(x, y)$.

Yet, when the fast dynamics is non-gradient, the matrix-vector multiplication $(DF(x))^T w$, in particular $C(x, y)^T w$, will impose a very severe computational challenge in this rather general situation, because it is not possible to apply the trick of directional derivative. We do not have any perfect solution for this non-gradient case and the numerical evaluation of the derivatives is probably the only method. For $DF = \overline{D_x f} + \overline{C}$, we assume that the full matrix $D_x f(x, y)$ has an expression to compute and its transpose $(D_x f(x, y))^T$ is obtained by a numerical transpose operation. The term

$$\overline{C^T w} = \int \theta(x, y) \nabla_x \rho(x, y) dy \quad \text{where } \theta(x, y) \doteq \langle f(x, y), w \rangle,$$

will have to be approximated by numerical derivative of ρ :

$$\partial_{x_j} \rho(x, y) = \lim_{h \rightarrow 0} (\rho(x + h e_j, y) - \rho(x, y)) / h, \quad j = 1, \dots, m \quad (20)$$

where e_j is the unit vector along x_j axis. Then the j -th component is

$$(\overline{C^T w})_j = \lim_{h \rightarrow 0} \int \theta(x, y) (\rho(x + h e_j, y) - \rho(x, y)) / h dy$$

By choosing a finite number $h \ll 1$, this brute-force calculation will have to add m independent fast processes \tilde{Y}^{x+he_j} , $j = 1, \dots, m$, to account for $\rho(x + h e_j, \cdot)$. The scheme (20) is computationally feasible only when the dimension of \mathcal{X} is low. In the next subsection, we show that the x -derivative of $\nabla_x \rho$ can be transformed to the y -derivative of some function by the perturbation analysis for the equilibrium density $\rho(x, y)$. However, the numerical challenge in this new form still exists.

2.5. Connection with the central limit theorem. In the last part of this section, we give a remark on the connection with the normal deviation from the averaged system. In the MsGAD, the Jacobi $DF(x)$ is important: It determines the linearization of the averaged dynamics F . This linearization also plays an important role in approximating $X^\varepsilon - \bar{X}$, the difference of the solutions to (1) and (5). Define the normalized difference

$$\xi_t^\varepsilon \doteq \frac{1}{\sqrt{\varepsilon}} (X_t^\varepsilon - \bar{X}_t) \quad (21)$$

By Theorem 3.1, §7.3 in [12], under the assumption of strong mixing, the normalized difference converges weakly to the solution of the SDE:

$$\dot{\xi}(t) = (DF(\bar{X}_t)) \xi(t) + \beta(\bar{X}_t) \eta(t) \quad (22)$$

where $DF(\bar{X}_t)$ is the Jacobi matrix DF at the averaged solution \bar{X} and the diffusion term β is $m \times m$ matrix such that

$$\beta(x) \beta(x)^T = A(x) \doteq \lim_{T \rightarrow \infty} \frac{1}{T} \int_0^T \int_0^T (f(x, \tilde{Y}_s^x) - F(x)) \otimes (f(x, \tilde{Y}_t^x) - F(x)) dt ds,$$

which can be easily estimated by running a long trajectory of the fast process.

If the formal asymptotic expansion is applied to derive the equation (22), the drift term in (22) has a different form, denoted as B ,

$$B(x) = \overline{D_x f}(x) + \int \left(\int_0^\infty \nabla_y E^y f(x, \tilde{Y}_\tau^x) d\tau \right) D_x b(x, y) \mu_x(dy) \quad (23)$$

where E^y is the expectation for the distribution of \tilde{Y}^x with initial $\tilde{Y}_0^x = y$. Refer to the appendix in [3] for this formula. Comparing (23) with (13), we find that $\overline{C}(x)$ should equal the double integral term on the right-hand side of (23). The proof of this fact is attached in the appendix of this paper. Numerically, the formula (23) is not friendly due to the differential operator ∇_y for the expectation term E^y .

In summary, the normalized difference ξ in (22) in the central limit theorem shares the same drift flow as our dynamics for the right direction v in (9). Hence, the numerical methods we developed here for the MsGAD may be useful to the calculation of ξ .

3. THE MSGAD FOR GRADIENT SYSTEM

As mentioned earlier, one important example of the slow-fast system (1) in practice is the extended Lagrangian method for the coarse-grained molecular dynamics. In this example, there exists an energy potential $U(x, y)$ in the extended space $\mathcal{X} \times \mathcal{Y}$ to drive the slow-fast system. For this gradient system, we shall see that the averaged system $\dot{\bar{X}} = F(\bar{X})$ is also a gradient system, i.e., there exists a (free energy) function $W(x)$ in \mathcal{X} such that $F(x) = \nabla W(x)$. The general discussions for the GAD above can be simplified much for this gradient case. The multiscale system (1) thus has a special form

$$\begin{cases} \dot{X}^\varepsilon = -\nabla_x U(X^\varepsilon, Y^\varepsilon), & (24a) \\ \dot{Y}^\varepsilon = -\frac{1}{\varepsilon} \nabla_y U(X^\varepsilon, Y^\varepsilon) + \frac{1}{\sqrt{\varepsilon}} \sigma \eta(t), & (24b) \end{cases}$$

where σ is assumed a scalar constant and η is a standard white noise. $U(x, y)$ is a potential energy function for $(X^\varepsilon, Y^\varepsilon)$. The equilibrium measure of the virtually fast process is

$$\mu_x(dy) = \rho(x, y) dy = \frac{1}{Z(x)} e^{-\frac{2}{\sigma^2} U(x, y)} dy, \quad Z(x) \doteq \int e^{-\frac{2}{\sigma^2} U(x, y)} dy. \quad (25)$$

As $\varepsilon \downarrow 0$, the averaged equation for \bar{X} is

$$\dot{\bar{X}} = F(\bar{X}), \quad (26)$$

where

$$F(x) = - \int \nabla_x U(x, y) \rho(x, y) dy.$$

By the definition of $Z(x)$, we can get

$$\nabla_x \log Z(x) = \frac{2}{\sigma^2} \int -\nabla_x U(x, y) \rho(x, y) dy = \frac{2}{\sigma^2} F(x),$$

Thus, the averaged equation (26) can be rewritten as a gradient system

$$\dot{\bar{X}} = -\nabla_x W(\bar{X}), \quad (27)$$

where the effective potential is

$$W(x) = -\frac{\sigma^2}{2} \log Z(x) = -\frac{\sigma^2}{2} \log \left(\int e^{-2U(x, y)/\sigma^2} dy \right). \quad (28)$$

By the calculation of (13), the Hessian matrix of $W(x)$ is

$$\nabla_x^2 W(x) = -DF(x) = \overline{\nabla_x^2 U}(x) - \frac{2}{\sigma^2} \overline{\nabla_x U} \otimes \overline{\nabla_x U}(x) + \frac{2}{\sigma^2} \overline{\nabla_x U}(x) \otimes \overline{\nabla_x U}(x). \quad (29)$$

The right hand side contains the Fisher information matrix of the invariant measure $\mu_x (= \rho(x, y) dy)$:

$$-E_{\mu_x} [\nabla_x^2 \log \rho] = \frac{4}{\sigma^2} (\overline{\nabla_x U} \otimes \overline{\nabla_x U}(x) - \overline{\nabla_x U}(x) \otimes \overline{\nabla_x U}(x)).$$

3.1. example. The following extended potential is widely used in free energy sampling and coarse-grained molecular dynamics simulation [32]:

$$U(x, y) = V(y) + \frac{1}{2} \kappa |x - q(y)|^2, \quad (30)$$

where $q = (q_1(y), \dots, q_n(y))$ is a given function mapping fast variables in \mathcal{Y} to the space \mathcal{X} , which defines coarse-grained variables. $\kappa > 0$ is a parameter coupling the potential of the microscopic system and the coarse-grained variables. Ideally, κ should be infinitely large, but it is a large constant in practice. The slow-fast dynamic system associated with (30) is

$$\begin{cases} \dot{X}^\varepsilon = -\kappa(X^\varepsilon - q(Y^\varepsilon)), & (31a) \\ \dot{Y}^\varepsilon = -\frac{1}{\varepsilon} \left(\nabla V(Y^\varepsilon) - \kappa(Dq(Y^\varepsilon))^\top (X^\varepsilon - q(Y^\varepsilon)) \right) + \frac{1}{\sqrt{\varepsilon}} \sigma \eta(t). & (31b) \end{cases}$$

where $Dq(y)$ is the Jacobi matrix $(\partial_{y_j} q_i)$. In order to sample the space \mathcal{X} with the correct marginal equilibrium distribution in the extended Lagrangian method., the slow dynamics (31a) actually should also be independently driven by an Brownian motion. Since here we only study the saddle point rather than the distribution of X , we only concern the deterministic steepest descent drift flow in (31a).

For this example, we have that $\nabla_x U(x, y) = \kappa(x - q(y))$ and $\nabla_x^2 U(x, y) \equiv \kappa I$ where I is the identity matrix. It follows that $\overline{\nabla_x U} = \kappa(\bar{x} - Q(x))$ and $\overline{\nabla_x^2 U} \equiv \kappa I$ where

$$\bar{x} = \int x \rho(x, y) dy, \quad Q(x) \doteq \bar{q}(x) = \int q(y) \rho(x, y) dy,$$

and

$$\rho(x, y) = Z(x)^{-1} e^{-\frac{2}{\sigma^2}V(y)} e^{-\frac{\kappa}{\sigma^2}(x-q(y))^2}.$$

Then, the effective potential W is

$$W(x) = -\frac{\sigma^2}{2} \log Z(x) = -\frac{\sigma^2}{2} \log \left(\int e^{-\frac{2}{\sigma^2}V(y)} e^{-\frac{\kappa}{\sigma^2}(x-q(y))^2} dy \right).$$

and the effective force for the slow variable is

$$F(x) = -\nabla_x W(x) = -\kappa(\bar{x} - Q(x)).$$

The Hessian matrix of W for this example, by the result in (29), is

$$\nabla_x^2 W(x) = \kappa I - \frac{2\kappa^2}{\sigma^2} \left(\overline{\langle x - q \rangle \otimes (x - q)}(x) - (\bar{x} - Q(x)) \otimes (\bar{x} - Q(x)) \right) \quad (32)$$

and hence

$$(\nabla_x^2 W)v = \kappa v - \frac{2\kappa^2}{\sigma^2} \left(\overline{\langle x - q, v \rangle (x - q)} - \langle \bar{x} - Q, v \rangle (\bar{x} - Q) \right).$$

The dynamics for direction v in the GAD, $\gamma\dot{v} = -(\nabla^2 W)v + \alpha v$, is

$$\gamma\dot{v} = \frac{2\kappa^2}{\sigma^2} \left(\overline{\langle x - q, v \rangle (x - q)} - \langle \bar{x} - Q(x), v \rangle (\bar{x} - Q(x)) \right) + \alpha'v$$

by absorbing the term κ into the new Lagrangian multiplier α' .

In summary, for this example, the GAD for the averaged system is

$$\begin{cases} \dot{x}(t) = -\kappa(\bar{x} - Q(x)) + 2 \frac{\langle \kappa(\bar{x} - Q(x)), v \rangle}{\langle v, v \rangle} v, & (33a) \\ \gamma\dot{v}(t) = \frac{2\kappa^2}{\sigma^2} \left(\overline{\langle x - q, v \rangle (x - q)} - \langle \bar{x} - Q(x), v \rangle (\bar{x} - Q(x)) \right) + \alpha'v. & (33b) \end{cases}$$

If let $\kappa \rightarrow \infty$, then $\rho(x, y) \rightarrow \tilde{Z}(x)^{-1} \delta(x - q(y)) e^{-\frac{2}{\sigma^2}V(y)}$ where $\tilde{Z}(x) \doteq \int \delta(x - q(y)) e^{-\frac{2}{\sigma^2}V(y)} dy$. And it follows that $W(x) \rightarrow \mathcal{F}(x) \doteq -\frac{\sigma^2}{2} \log \tilde{Z}(x)$ (up to a constant) where \mathcal{F} is the free energy surface of the coarse-grained variable x . For further details on the GAD for this type of question and the applications in coarse-grained molecular dynamics simulation, refer to the publication [29].

3.2. The dimer method for gradient system. The GAD for the gradient system (27) requires the calculation of the multiplication of Hessian $\nabla_x^2 W$ and vector v , which can be numerically approximated by the finite difference scheme when the Hessian itself is difficulty to obtain. This idea has been widely used in the dimer method ([16, 33]). The one-side finite difference scheme is

$$(\nabla_x^2 W)v \approx \frac{\nabla_x W(x + hv) - \nabla_x W(x)}{h} = -\frac{F(x + hv) - F(x)}{h}.$$

To evaluate $F(x + hv)$, which is $\int f(x + hv, y) \rho(x + hv, y) dy$, one simple approach is to run a second independent fast process \tilde{Y}_t^{x+hv} to obtain the density $\rho(x + hv, \cdot)$ parametrized at $x + hv$. When the central finite difference scheme is used,

the third process for $x - hv$ is required. This approach leads to an undesired extra burden of simulating multiple fast processes. In contrast, by using the formula derived in (29), only one trajectory for the virtually fast process is required.

4. NUMERICAL EXAMPLES

To illustrate how the MsGAD we have proposed works, we present two numerical examples below. The first is a system consisting of a two dimensional ordinary differential equation and a two dimensional stochastic ordinary differential equation. It is not a gradient system. We apply the HMM (Section 2.2.1) in the MsGAD. The second is a system of an Allen-Cahn partial differential equation and a stochastic Allen-Cahn partial differential equation. This second system has an extended potential functional. We apply and compare both the HMM and the seamless coupling scheme (Section 2.2.2) to this second example.

4.1. A two-dimensional example. We consider the following system on $\mathcal{X} \times \mathcal{Y} = \mathbb{R}^2 \times \mathbb{R}^2$

$$\begin{cases} \dot{X}_i = - \sum_{ij} D_{ij} X_j + Y_i^2, & (34a) \\ \dot{Y}_i = - \frac{1}{\varepsilon} \frac{Y_i}{\Gamma_i(X)} + \frac{1}{\sqrt{\varepsilon}} \sigma \eta(t). & (34b) \end{cases}$$

The vector field $\Gamma(x) = (\Gamma_1(x), \Gamma_2(x)) : \mathcal{X} \rightarrow \mathcal{Y}$ is given. $D = (D_{ij})$ is a 2×2 symmetric matrix. σ is a constant.

The processes $\{Y_i(t)\}$ are independent Ornstein-Uhlenbeck processes parametrized by $X = x$. The equilibrium distribution of $Y = (Y_1, Y_2)$ is the product measure of $\mathcal{N}(0, \sigma^2 \Gamma_i(x)/2)$. The calculation shows that the limit equation has a closed form

$$\dot{\bar{X}}_i = - \sum_{ij} D_{ij} \bar{X}_j + \frac{\sigma^2}{2} \Gamma_i(\bar{X}). \quad (35)$$

Note that (34a) can be rewritten as $\dot{X} = -\nabla_X(\frac{1}{2}X^\top DX - \sum_i Y_i^2 X_i)$ and (34b) also equals to $-\nabla_Y(\sum_i \frac{Y_i^2}{2\Gamma_i(X)})$. However, it is easy to see that there is no single potential for (34) in the extended space $\mathcal{X} \times \mathcal{Y}$, for whatever choice of Γ . This means that we do not know *a priori* if the averaging system is gradient or not. The analytical form of the averaged system (35) shows that it is gradient if and only if the vector field Γ is gradient, i.e., there exists a scalar function R such that

$$\Gamma(x) = (\Gamma_1(x), \dots, \Gamma_n(x)) = \nabla_x R(x). \quad (36)$$

This suggests that the existence of an extended potential function is a sufficient, but not a necessary condition for the averaged dynamics to be gradient.

In the next, we show the numerical results of the MsGAD for this example. First, we have to run the both directions $v(t)$ and $w(t)$ in our MsGAD scheme, because, as we just mentioned, we do not know DF is symmetric *a priori*. To validate our result, we not only show the convergence to the saddle point, but also compare the trajectory $x(t)$ in the MsGAD with that of the classic GAD applied to the known limit equation (35). The parameters we used in the numerical tests are the following. $\sigma^2 = 10$, $D = \begin{bmatrix} 0.8 & -0.2 \\ -0.2 & 0.5 \end{bmatrix}$, and for $x = (x_1, x_2)$

$$R(x) = \sum_i \arctan(x_i - 5), \quad \Gamma_i(x) = (1 + (x_i - 5)^2)^{-1}, \quad i = 1, 2.$$

The averaged equation (35) becomes

$$\dot{\bar{X}} = -\nabla W(\bar{X}), \quad \text{where } W(x) = x^\top D x - \frac{\sigma^2}{2} R(x). \quad (37)$$

W has three local minima $m_1 = (0.4643, 0.6985)$, $m_2 = (2.2038, 5.9804)$, $m_3 = (5.7109, 6.2369)$ and two saddle points $s_1 = (3.5689, 6.0735)$, $s_2 = (1.2841, 3.4483)$. See Figure 1 below.

In the HMM scheme of the MsGAD, we use the forward Euler solver for the whole system. We take the macro- time step size $\Delta t = 0.01$ for both x^ε and $v^\varepsilon, w^\varepsilon$ and set $\tau = 1.0$ and $K = 1$ for this example. The micro- time step size is $\delta\tau = \varepsilon \times 0.01$ and the total sampling time $T = 10$ is used to estimate the effective force and the Jacobi matrix. The initial values for x are set on three local minima, respectively. The initial values for the directions (v, w) and the fast processes are arbitrarily chosen. Figure 1 shows the four GAD trajectories of the x component (dashed line) starting from three local minima. Depending on the initial values of x , these four trajectories converge to the different neighboring saddle points. Two of them which start from m_2 , converge to the saddle point s_1 and s_2 respectively, due to the different initial values for the directions v and w .

4.2. A coupled Allen-Cahn system. Our second example is a system of stochastic partial differential equations of $(u^\varepsilon(x, t), \phi^\varepsilon(x, t))$ in the Hilbert space $L^2([0, 1])$, satisfying Allen-Cahn-type equations with Neumann boundary condition:

$$\begin{cases} \partial_t u^\varepsilon = \kappa^2 \Delta u^\varepsilon + u^\varepsilon - (u^\varepsilon)^3 + \mu \phi^\varepsilon, & (38a) \\ \partial_t \phi^\varepsilon = \frac{1}{\varepsilon} [\Delta \phi^\varepsilon - \phi^\varepsilon + \mu u^\varepsilon] + \frac{\sigma}{\sqrt{\varepsilon}} \dot{W}(t), & (38b) \end{cases}$$

where $\Delta = \partial_x^2$ and $W(t)$ is an $L^2([0, 1])$ -valued Wiener process with trace class (spatial) covariance operator Q . \dot{W} is white in time. κ is the diffusion coefficient in slow dynamics and μ is the coupling constant between

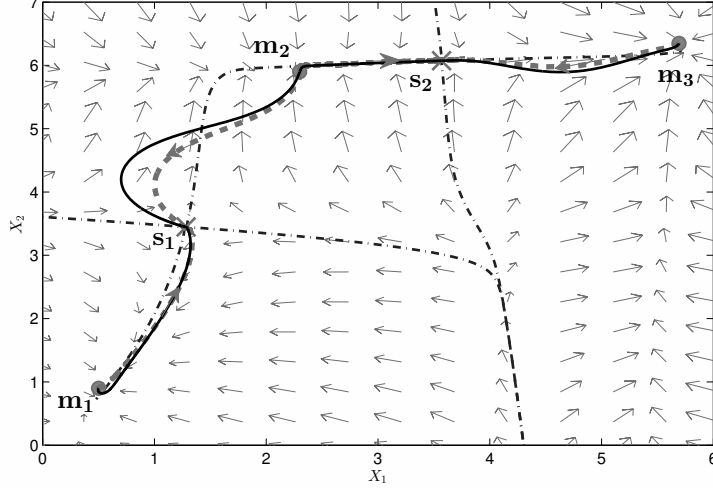


FIGURE 1. GAD trajectories from three different local minima (m_1, m_2 and m_3) to two different saddle points (s_1 and s_2). The flow indicated by the arrows corresponds to the averaged gradient system (37). The dash-dotted curves are the stable/unstable manifolds of the two saddle points; they determine the basin boundaries of the three local wells. The thick dashed curves with arrows marked are the trajectories of MsGAD by the HMM. As comparison, the thin solid curves are the trajectories of the GAD directly applied to the closed form (37) of the averaged system.

the slow and fast dynamics. σ is the noise intensity. For any fixed $u^\varepsilon = u$, the equilibrium distribution of the SPDE (38b) is the Gaussian measure $\mathcal{N}(\mu(I - \Delta)^{-1}u, \sigma^2(I - \Delta)^{-1}Q/2)$ on the Cameron–Martin space. We simply choose Q as identity, i.e., formally, \dot{W} is the spatio-temporal white noise. Then, it is easy to see that the averaged equation for the limit solution \bar{u} is

$$\begin{cases} \partial_t \bar{u} = \kappa^2 \Delta \bar{u} + \bar{u} - \bar{u}^3 + \mu^2 (I - \Delta)^{-1} \bar{u}, & (39a) \\ \frac{\partial \bar{u}}{\partial \bar{n}} \Big|_{x=0} = 0, \quad \frac{\partial \bar{u}}{\partial \bar{n}} \Big|_{x=1} = 0. & (39b) \end{cases}$$

In this example, we can find an energy functional $U(u, \phi)$ jointly for the pair (u, ϕ) :

$$U(u, \phi) = \int_{\Omega} \frac{\kappa^2}{2} u_x^2 + \frac{1}{4} (u^2 - 1)^2 - \mu u \phi + \frac{1}{2} \phi_x^2 + \frac{1}{2} \phi^2 \, dx. \quad (40)$$

Since this is a gradient system, the corresponding MsGAD only involves one direction (see Section 3):

$$\begin{cases} \partial_t u^\varepsilon = -\delta_u U(u^\varepsilon, \phi^\varepsilon) + 2 \frac{\langle \delta_u U(u^\varepsilon, \phi^\varepsilon), v^\varepsilon \rangle}{\langle v^\varepsilon, v^\varepsilon \rangle} v^\varepsilon, & (41a) \\ \partial_t \phi^\varepsilon = -\frac{1}{\varepsilon} \delta_\phi U(u^\varepsilon, \phi^\varepsilon) + \frac{\sigma}{\sqrt{\varepsilon}} \dot{W}(t), & (41b) \\ \partial_t v^\varepsilon = -\delta_u^2 U(u^\varepsilon, \phi^\varepsilon) v^\varepsilon + C v^\varepsilon - \alpha^\varepsilon v^\varepsilon, & (41c) \end{cases}$$

where $\delta_u U$ and $\delta_\phi U$ are the Fréchet derivative of $U(u, \phi)$. $\delta_u^2 U$ is the Hessian. Here C is $-\frac{2}{\sigma^2} \delta_u U \otimes \delta_u U + \frac{2}{\sigma^2} \overline{\delta_u U} \otimes \overline{\delta_u U}$.

The equation (41) are solved by the HMM and the seamless coupling method. The parameters are $\kappa = 0.01$, $\mu = 1$ and $\sigma = 0.3$. The time-discretization scheme for the equation (41a) is a convex-splitting scheme for saddle point search ([15]) to allow a larger stable time step size Δt . The spatial discretization is finite difference method with uniform mesh grid size $\Delta x = 1/200$. The term $\delta_u^2 U(u, \phi)v$ in (41) is calculated by finite difference approximation

$$\delta_u^2 U(u, \phi)v = \frac{1}{h} [\delta_u U(u + hv, \phi) - \delta_u U(u, \phi)]$$

with $h = 0.001$. In the HMM, the macro- time step size for u^ε and v^ε is $\Delta t = 0.025$ and the micro- time step size for ϕ^ε is $\delta t = 0.01 \times \varepsilon$. In the test, 10000 are used for the sampling time T to estimate averaged quantities. The initial state is the saddle point for $\mu = 0$ (dashed lines in Figure 2), obtained by the traditional GAD for the dynamics (38a) with $\mu = 0$. At $\mu = 1$, the obtained saddle point from the HMM–MsGAD is plotted in Figure 2. As a comparison, this figure also shows the numerical result (marked by cross signs) obtained from the closed form for averaged system (39). These two results shows no difference in this plot.

For the seamless coupling method to solve the MsGAD (41), according to Section 2.2.2, the boosted system is

$$\begin{cases} \partial_t u^\varepsilon = -\delta_u U(u^\varepsilon, \phi^\varepsilon) + 2 \frac{\langle \delta_u U(u^\varepsilon, \phi^\varepsilon), v^\varepsilon \rangle}{\langle v^\varepsilon, v^\varepsilon \rangle} v^\varepsilon, & (42a) \\ \partial_t \phi^\varepsilon = -\frac{1}{\varepsilon \lambda} \delta_\phi U(u^\varepsilon, \phi^\varepsilon) + \frac{\sigma}{\sqrt{\varepsilon \lambda}} \dot{W}_1(t), & (42b) \\ \partial_t \psi^\varepsilon = -\frac{1}{\varepsilon \lambda} \delta_\psi U(u^\varepsilon, \psi^\varepsilon) + \frac{\sigma}{\sqrt{\varepsilon \lambda}} \dot{W}_2(t), & (42c) \\ \partial_t v^\varepsilon = -\delta_u^2 U(u^\varepsilon, \phi^\varepsilon) v^\varepsilon + f(u^\varepsilon, \phi^\varepsilon) \langle g(u^\varepsilon, \phi^\varepsilon), v^\varepsilon \rangle \\ \quad - f(u^\varepsilon, \psi^\varepsilon) \langle g(u^\varepsilon, \psi^\varepsilon), v^\varepsilon \rangle - \alpha^\varepsilon v^\varepsilon, & (42d) \end{cases}$$

where W_1 and W_2 are two iid copies of W . $\langle \cdot, \cdot \rangle$ is the inner product in $L^2([0, 1])$. Choose $\varepsilon = 1.0 \times 10^{-4}$ and $\lambda = 10$ (or effectively, $\varepsilon \lambda = 1.0 \times 10^{-3}$). The simulation uses the same time step size $\tilde{\Delta} t = 1.0 \times 10^{-3}$ for all components.

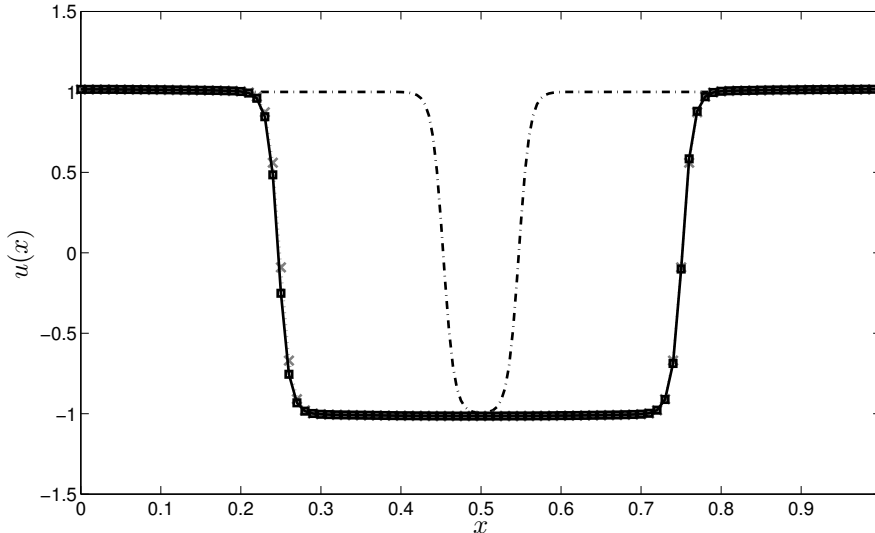


FIGURE 2. The saddle points at $\mu = 0$ (dash-dotted line) and $\mu = 1$ (two superimposed solid lines). In the two solid lines, the square marks (' \square ') are from the MsGAD by solving the equation (41) and the cross marks (' \times ') are from the traditional GAD applied to the system (39). A positive μ increases the width of the nuclei shape.

The same initial state as in the HMM is used. The obtained profile of the saddle point is not visually distinguishable from the result of the HMM presented in Figure 2. So we do not plot it again.

We also investigated the process of convergence from the same initial state in the HMM and the seamless coupling method for the MsGAD. Define the error at time t ,

$$\text{err}_H(t) = \|u_H(x, t) - u^*(x)\|_{L^2}, \quad \text{err}_S(t) = \|u_S(x, t) - u^*(x)\|_{L^2},$$

where $u_H(x, t)$ represents the result of (41) solved by the HMM and $u_S(x, t)$ is the result of (42) solved by seamless coupling method. The true solution $u^*(x)$ is obtained from the classic GAD for the closed form of averaged system (39) with very fine time step size. Figure 3 plots the time evolution of the two errors $\text{err}_H(t)$ and $\text{err}_S(t)$, which shows that the decay for the HMM error is faster than the seamless coupling method. However, this does not mean that the HMM is more efficient since the HMM involves very expensive samplings at each macro- time step. In fact, to obtain the HMM error curve in Figure 3, it took more than 70 CPU hours, while for the seamless coupling result, it took less than two minutes on the same computer!

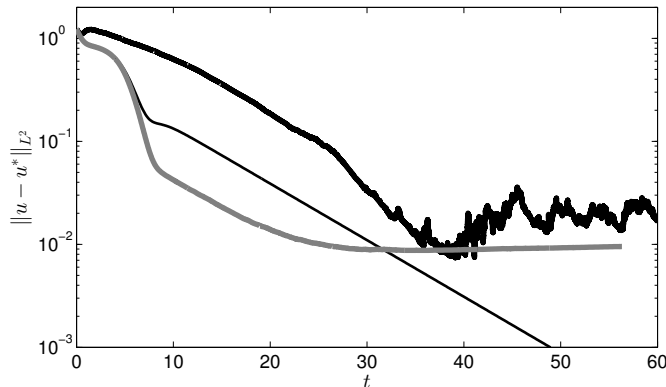


FIGURE 3. The evolution of the errors with time. The thinner line is from the classic GAD applied on the averaged system(39). The other two thicker lines are from the HMM (grey line) and from the seamless coupling method (dark line), respectively.

5. CONCLUSION

We have investigated the multiscale method for the GAD in slow-fast systems. In order to calculate saddle point of effective dynamics, we proposed a new slow-fast system, the MsGAD, whose effective dynamics is consistent with the GAD for the effective dynamics. By applying the multiscale numerical method such as the HMM or the seamless coupling method, we efficiently explore saddle points on averaged dynamics. Such saddle points are useful to help understand the non-equilibrium behaviours of the slow dynamics. There are a few questions remaining on fluctuations and transitions in slow-fast stochastic dynamic systems, besides the exploration of index-1 saddle point for effective dynamics. In this ending time of writing this article, we note an interesting result in [18] that the traditional HMM has been modified by using multiple replica of fast process in order to correctly capture the fluctuations in direct simulation. This technique would offer a tool to numerically validate immediate relevance of saddle point to noise-induced transitions in stochastic slow-fast system.

APPENDIX: PROOF OF (23).

To show that B is the Jacobi matrix DF , we just need to prove that

$$\begin{aligned} & \int (f(x, y) - F(x)) \otimes \nabla_x \log \rho(x, y) \rho(x, y) (dy) \\ &= \int \left(\int_0^\infty \nabla_y E^y f(x, \tilde{Y}_\tau^x) d\tau \right) D_x b(x, y) \rho(x, y) dy. \end{aligned}$$

To show this matrix equality, we just need to show

$$\begin{aligned} & \int (f(x, y) - F(x)) \langle \nabla_x \rho(x, y), e \rangle dy \\ &= \int \left(\int_0^\infty \nabla_y \mathbb{E}^y f(x, \tilde{Y}_\tau^x) d\tau \right) (D_x b(x, y)) e \rho(x, y) dy \end{aligned}$$

for arbitrary vector e . Write the infinitesimal perturbation $\tilde{\rho} := \rho(x + he, y) - \rho(x, y) \approx h \nabla_x \rho(x, y) \cdot e$ and $\tilde{b}(x, y) = b(x + he, y) - b(x, y) \approx h(D_x b(x, y))e$ for $h \ll 1$, and assume a is independent of x , then the lemma below tells us that

$$\int (f(x, y) - F(x)) \langle \nabla_x \rho(x, y), e \rangle dy = - \int \langle \nabla_y u, (D_x b(x, y))e \rangle \rho(x, y) dy$$

where u satisfies $\mathcal{L}_y u(x, y) = f(x, y) - F(x)$. By the Feymann-Kac formula, we have the representation $u(x, y) = \int_0^\infty \mathbb{E}^y[-f(x, \tilde{Y}_t^x) + F(x)] dt$, so $\nabla_y u = - \int_0^\infty \nabla_y \mathbb{E}^y[f(x, \tilde{Y}_t^x)] dt$. This completes our proof.

Lemma 1. *If $\rho(y)$ is the unique equilibrium probability density function of the SDE*

$$dY = b(Y)dt + \sigma(Y)dW,$$

\mathcal{L} is the infinitesimal generator, and the infinitesimal perturbation is applied for the drift term: $b \rightarrow b + \tilde{b}$ and the diffusion term $a \doteq \sigma \sigma^T \rightarrow a + \tilde{a}$, where \tilde{b} and \tilde{a} are small terms, and let $\Theta \doteq \int \theta(y) \rho(y) dy$, then the perturbation of Θ is

$$\delta\Theta \doteq \int \theta(y) \tilde{\rho}(y) dy = - \int \tilde{b} \cdot (\rho \nabla u)(y) dy - \frac{1}{2} \int \tilde{a} : \rho \nabla \nabla u(y) dy.$$

where u is the solution of the adjoint equation $\mathcal{L}u = \theta(y) - \Theta$ and decays to 0 at infinity.

Proof. The infinitesimal generator is $\mathcal{L} = b(y) \cdot \nabla + \frac{1}{2} a(y) : \nabla \nabla$. The density ρ satisfies the equation $\mathcal{L}^* \rho = 0$ where \mathcal{L}^* is the adjoint of \mathcal{L} . By linearizing the perturbed equation, we have $\mathcal{L}^* \tilde{\rho} = \nabla \cdot (\rho \tilde{b}) - \nabla \nabla : (\rho \tilde{a})$. Multiply this equation by u , then from the integration parts, we have $\delta\Theta = \int \tilde{\rho}(y) \theta(y) dy = \int \tilde{\rho}(y) \mathcal{L}u dy = - \int \tilde{b} \cdot (\rho \nabla u)(y) dy - \frac{1}{2} \int \tilde{a} : \rho \nabla \nabla u(y) dy$. \square

REFERENCES

- [1] Josep Maria Bofill and Wolfgang Quapp. The variational nature of the gentlest ascent dynamics and the relation of a variational minimum of a curve and the minimum energy path. *Theoretical Chemistry Accounts*, 135(1):1–14, 2015.
- [2] Josep Maria Bofill, Wolfgang Quapp, and Efreem Bernuz. Some remarks on the model of the extended gentlest ascent dynamics. *Journal of Mathematical Chemistry*, 53(1):41–57, 2014.
- [3] F. Bouchet, T. Grafke, T. Tangarife, and E. Vanden-Eijnden. Large deviations in fast-slow systems. *arXiv:1510.02227v1*.
- [4] G. M. Crippen and H. A. Scheraga. Minimization of polypeptide energy : XI. the method of gentlest ascent. *Arch. Biochem. Biophys.*, 144(2):462–466, 1971.
- [5] W. E, W. Ren, and E. Vanden-Eijnden. String method for the study of rare events. *Phys. Rev. B*, 66:052301, 2002.

- [6] Weinan E. *Principle of Multiscale Modeling*. Cambridge University Press, 2011.
- [7] Weinan E and Bjorn Engquist. The heterogeneous multiscale methods. *Commun. Math. Sci.*, 1(1):87–132, 03 2003.
- [8] Weinan E, Bjorn Engquist, Xiantao Li, Weiqing Ren, and Eric Vanden-Eijnden. The heterogeneous multiscale method: A review. *Commun. Comput. Phys.*, page 2007, 2007.
- [9] Weinan E, Weiqing Ren, and Eric Vanden-Eijnden. A general strategy for designing seamless multiscale methods. *Journal of Computational Physics*, 228(15):5437 – 5453, 2009.
- [10] Weinan E and Xiang Zhou. The gentlest ascent dynamics. *Nonlinearity*, 24(6):1831, 2011.
- [11] Weinan E, Xiang Zhou, and Xiuyuan Cheng. Subcritical bifurcation in spatially extended systems. *Nonlinearity*, 25:761, 2012.
- [12] M. I. Freidlin and A. D. Wentzell. *Random Perturbations of Dynamical Systems*. Grundlehren der mathematischen Wissenschaften. Springer-Verlag, New York, 3 edition, 2012.
- [13] Weiguao Gao, Jing Leng, and Xiang Zhou. An iterative minimization formulation for saddle point search. *SIAM J. Numer. Anal.*, 53(4):1786–1805, 2015.
- [14] Weiguao Gao, Jing Leng, and Xiang Zhou. Iterative minimization algorithm for efficient calculations of transition states. *Journal of Computational Physics*, 309:69 – 87, 2016.
- [15] Shuting Gu and Xiang Zhou. Convex splitting strategy for saddle point calculation for phase field models. *in preparation*, 2016.
- [16] G. Henkelman and H. Jónsson. A dimer method for finding saddle points on high dimensional potential surfaces using only first derivatives. *J. Chem. Phys.*, 111(15):7010–7022, 1999.
- [17] Marcella Iannuzzi, Alessandro Laio, and Michele Parrinello. Efficient exploration of reactive potential energy surfaces using Car-Parrinello molecular dynamics. *Phys. Rev. Lett.*, 90:238302, Jun 2003.
- [18] D. Kelly and E. Vanden-Eijnden. Fluctuations in the heterogeneous multiscale methods for fast-slow systems. *arXiv:1601.02147*.
- [19] R. Z. Khasaminskii. A limit theorem for the solutions of differential equations with random right-hand sides. *Theory of Probability & Its Applications*, 11(3):390–406, 1966.
- [20] Rafail Z. Khasminkii and George Yin. On averaging principles: An asymptotic expansion approach. *SIAM Journal on Mathematical Analysis*, 35(6):1534–1560, 2004.
- [21] P.E. Kloeden and E. Platen. *Numerical Solution of Stochastic Differential Equations*. Stochastic Modelling and Applied Probability. Springer Berlin Heidelberg, 2013.
- [22] Alessandro Laio and Michele Parrinello. Escaping free-energy minima. *Proceedings of the National Academy of Sciences*, 99(20):12562–12566, 2002.
- [23] Benedict Leimkuhler, Charles Matthews, and Gabriel Stoltz. The computation of averages from equilibrium and nonequilibrium langevin molecular dynamics. *IMA Journal of Numerical Analysis*, 36(1):13–79, 2016.
- [24] Chen Li, Jianfeng Lu, and Weitao Yang. Gentlest ascent dynamics for calculating first excited state and exploring energy landscape of Kohn-Sham density functionals. *The Journal of Chemical Physics*, 143(22):224110, 2015.
- [25] L. Maragliano, A. Fischer, E. Vanden-Eijnden, and G. Ciccotti. String method in collective variables: Minimum free energy paths and isocommittor surfaces. *J. Chem. Phys.*, 125(2):024106, 2006.
- [26] N. Mousseau and G.T. Barkema. Traveling through potential energy surfaces of disordered materials: the activation-relaxation technique. *Phys. Rev. E*, 57:2419, 1998.
- [27] George Papanicolaou. Introduction to the asymptotic analysis of stochastic equations. In *Lectures in Appl. Math.* Amer. Math. Soc.
- [28] A. Samanta and W. E. Atomistic simulations of rare events using gentlest ascent dynamics. *J. Chem. Phys.*, 136:124104, 2012.

- [29] Amit Samanta, Ming Chen, Tang-Qing Yu, Mark Tuckerman, and Weinan E. Sampling saddle points on a free energy surface. *The Journal of Chemical Physics*, 140(16):164109, 2014.
- [30] A.Yu. Veretennikov. On large deviations for SDEs with small diffusion and averaging. *Stoch. Proc. Appl.*, 89(1):69–79, 2000.
- [31] D. J. Wales. *Energy Landscapes with Application to Clusters, Biomolecules and Glasses*. Cambridge University Press, 2003.
- [32] E. Weinan and Eric Vanden-Eijnden. Metastability, conformation dynamics, and transition pathways in complex systems. In Sabine Attinger and Petros Koumoutsakos, editors, *Multiscale Modelling and Simulation*, volume 39 of *Lecture Notes in Computational Science and Engineering*, pages 35–68. Springer Berlin Heidelberg, 2004.
- [33] J. Zhang and Q. Du. Shrinking dimer dynamics and its applications to saddle point search. *SIAM J. Numer. Anal.*, 50:1899–1921, 2012.
- [34] Xiang Zhou. *Noise-induced Transition Pathway in Non-gradient Systems*. PhD thesis, Princeton University, 2009.